given by

$$1+\hat{D}=\omega_{ex}\Omega/_0, \tag{A12}$$

where ω_{ex} is the exchange frequency. Straightforward integration gives

$$R\approx 6\hat{D}^{-1/2} \tag{A13}$$

for $\hat{D}\gg 1$. For the numerical examples here [see (69) and note that for an antiferromagnet (Sec. III) Ω_q^{-1} should be replaced by Ω_q^{-2} in R] R is safely small and (A8) may be used. In substances with high antisotropy, however, R can be comparable to unity and (A8) must accordingly be modified.[24]

[24] Tin Ngwe, D. Hone, V. Jaccarino, and P. Pincus (to be published) have independently concluded that R can be important. I am grateful to V. Jaccarino for a private communication on this matter.

By using (A8) and noting that, at infinite temperature,

$$\langle I_k^+ I_k^-\rangle = 2\langle I_k^z I_{-k}^z\rangle = \tfrac{2}{3}I(I+1), \tag{A14}$$

we obtain finally

$$\Phi_k(t)\approx 1-(\omega_n A)^2 N^{-1}\tfrac{1}{3}I(I+1)\sum_q \Omega_q^{-2} \times\int_0^t (t-\tau)\exp[i(\omega_k-\omega_q)\tau]d\tau \tag{16}$$

to second order in $\omega_n A$. The relation

$$\int_0^t dt'\int_0^{t'} dt''\exp[i\omega(t'-t'')]=\int_0^t (t-\tau)\exp(i\omega\tau)d\tau \tag{A15}$$

has been used in (16).

PHYSICAL REVIEW VOLUME 173, NUMBER 2 10 SEPTEMBER 1968

Nuclear-Magnetic-Resonance Studies of Mn^{55} in Ni–Mn Alloys

R. L. STREEVER
U.S. Army Electronics Command, Fort Monmouth, New Jersey 07703

(Received 28 February 1968)

The nuclear-magnetic-resonance line shapes of Mn^{55} have been studied in ferromagnetic Ni-rich Ni–Mn alloys with Mn concentrations of between 0.8 and 20.5 at.% Mn. Measurements were made at 4.2°K and over smaller concentration ranges at 77°K and room temperature by plotting the spin-echo amplitudes as a function of frequency across the inhomogeneously broadened nuclear resonance lines. Satellites are observed at low Mn concentrations at 4.2°K on both the high- and low-frequency sides of the dilute Mn in Ni line. A detailed analysis of the satellite structure is made by considering contributions to the hyperfine fields at the nuclei from the parent atom as well as from neighboring atoms, taking into account the antiferromagnetic interactions which exist in these alloys. In addition to the localized effects associated with the satellite structure, a shift of the dilute-Mn-in-Ni line is observed at low Mn concentrations which may be due to a long-range increase of moments on Mn atoms due to the addition of Mn. Studies made on a dilute (0.8 at.%) Mn-in-Ni alloy in external dc magnetic fields indicate the Mn^{55} hyperfine field to be negative.

I. INTRODUCTION

THE magnetic properties of the Ni–Mn alloy system have been extensively studied for several decades.[1–8] In the disordered Ni–Mn alloys, the magnetization rises at low concentrations of Mn, reaches a peak at around 10 at.% Mn, and then decreases quite rapidly to a relatively low value at about 30% Mn. As has been discussed by Marcinkowski and Poliak,[7] Carr,[9] Sato,[10] and others, this behavior is believed to be due to a competition between ferromagnetic and antiferromagnetic interactions in the Ni–Mn system. The Mn–Ni and Ni–Ni exchange interactions are believed to be ferromagnetic, while the Mn–Mn interactions are believed to be relatively large and antiferromagnetic. Consequently, for low concentrations of Mn in Ni, the Mn moments are aligned ferromagnetically. Since the Mn moment is about 3 Bohr magnetons (μ_B) compared with the Ni moment of 0.6 μ_B, an increase in magnetization occurs at low Mn concentrations. At higher concentrations when the Mn atoms begin to interact, the

[1] C. Sadron, Ann. Phys. (Paris) **17**, 371 (1932).
[2] S. Kaya and A. Kussmann, Z. Physik **72**, 293 (1931).
[3] S. Kaya and M. Nakayama, Proc. Phys. Math. Soc. Japan **22**, 126 (1940).
[4] G. R. Piercy and E. R. Morgan, Can. J. Phys. **31**, 529 (1953).
[5] J. S. Kouvel *et al.*, J. Appl. Phys. **29**, 518 (1958); J. Phys. Radium **20**, 198 (1959).
[6] A. Paoletti *et al.*, J. Appl. Phys. **37**, 3236 (1966).
[7] M. J. Marcinkowski and R. M. Poliak, Phil. Mag. **8**, 1023 (1963).
[8] H. C. VanElst *et al.*, Physica **28**, 1297 (1962).
[9] W. J. Carr, Jr., Phys. Rev. **85**, 590 (1952).
[10] H. Sato, in *Proceedings of the International Conference on Magnetism and Magnetic Materials* (American Institute of Electrical Engineers, New York, 1955), p. 119.

Mn moments tend to become paired off and a reduction in magnetization occurs. In the concentration range around Ni_3Mn, the alloys can exist in both atomically ordered and atomically disordered states. Since in the ordered alloys Mn atoms have only Ni nearest neighbors, the Mn moments are ferromagnetically aligned and the alloy becomes strongly ferromagnetic.

The nuclear magnetic resonance of Mn^{55} in Ni has been recently observed by Koi[11] in alloys containing 1 and 2% Mn. In the present work, we have used a spin-echo technique to study the nuclear magnetic resonance of Mn^{55} in Ni–Mn alloys with concentrations of up to 20.5 at.% Mn. We have determined the hyperfine-field distributions in these alloys by measuring the amplitude of the spin-echo signals as a function of frequency across the inhomogeneously broadened resonance lines. Preliminary results of this work have been reported previously.[12] In Sec. II experimental techniques are discussed briefly and experimental results presented. In Sec. III a discussion of the magnetic properties of the disordered Ni–Mn alloys is given. Hyperfine fields in these alloys are then discussed and a comparison of the nuclear-resonance results with recent hyperfine-field data[13,14] in Ni–Mn alloys from specific-heat measurements is made.

II. EXPERIMENTAL TECHNIQUES AND RESULTS

A. Samples

A series of Ni–Mn alloys containing 1.9, 4.8, 6.8, 9.8, 14.4, 20.5, and 25.5% Mn (all percentages atomic) were prepared by arc melting the appropriate amounts of the constituent metals. Since the crucibles used to prepare the samples were water cooled following melting, the samples reached room temperature quite quickly and it is believed that no appreciable ordering of the higher-concentration samples occurred, although the 25.5% sample probably exhibits some ordered phase. The ingots were then filed into fine powders of 50 μ or less in diameter. In order to prevent ordering of the higher-concentration alloys, no annealing of the powders was carried out. In addition to these alloys, a sample containing 0.8 at.% Mn in Ni was studied. This sample was prepared by atomizing the molten alloy into a fine spray and the resulting particle size was under 10 μ.

B. Equipment and Measuring Techniques

A variable-frequency spin-echo spectrometer operating in the 200–400-MHz frequency range was used for these studies. The essential parts of the spectrometer were a pulsed rf oscillator and a superheterodyne receiver. The equipment is similar in principle to that used previously[15,16] for studies in the lower frequency ranges and no detailed discussion will be given here. The 4.2° K measurements were made by use of an exposed-tip helium Dewar.

The measurements were made by plotting the amplitude of the spin-echo signals as a function of frequency across the inhomogeneously broadened resonance lines. Pulses of about 1 μsec in width were used. By adjusting the amplitudes of the rf pulses at each frequency to a maximum echo signal, we feel we have compensated for any variation in rf enhancement with frequency. The echo maximum occurred at relatively low power levels in the zero-field studies, and we believe that the signals observed are from nuclei in domain walls where the rf fields are strongly enhanced. The experimental echo amplitudes at each frequency were divided by the frequency squared to take into account the fact that the nuclear signal induced in the sample coil is proportional to the frequency and to account for the increased nuclear polarization at higher frequencies. Detailed discussions of the experimental methods and calibration techniques have been given previously.[15,16]

C. Experimental Results in Zero External Field

The Mn^{55} line shapes at 4.2°K corrected by the factor of ν^2 (ν being the frequency) are shown for the low-concentration alloys in Fig. 1 and for the higher-concentration alloys in Fig. 2. No measurements were made in the 25.5% alloy because of weak signals,

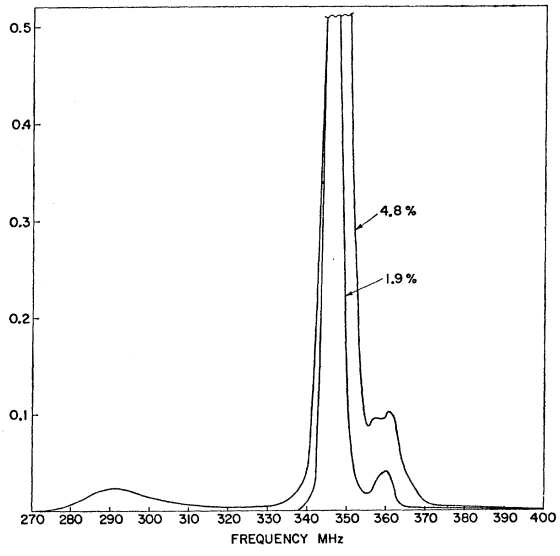

FIG. 1. The Mn^{55} line shapes at 4.2°K in the lower concentration Ni–Mn alloys. The line shapes have been corrected as explained in the text.

[11] Y. Koi and A. Tsujimura, J. Phys. Soc. Japan **18**, 1347 (1963).
[12] R. L. Streever, Bull. Am. Phys. Soc. **12**, 1043 (1967).
[13] W. Proctor *et al.*, Proc. Phys. Soc. (London) **90**, 697 (1967).
[14] P. N. Stetsenko and Y. I. Avksentev, Bull. Acad. Sci. USSR **30**, 1005 (1967).
[15] R. L. Streever and G. A. Uriano, Phys. Rev. **139**, A135 (1965).
[16] R. L. Streever and G. A. Uriano, Phys. Rev. **149**, 295 (1966).

probably due to the fact that this alloy is not strongly ferromagnetic. Results at 77°K are shown in Fig. 3 and at room temperature in Fig. 4. At room temperature in concentrations above 9.8% the signal-to-noise ratio was too poor to make measurements. In Fig. 5 the frequencies of the peak of the main resonance line

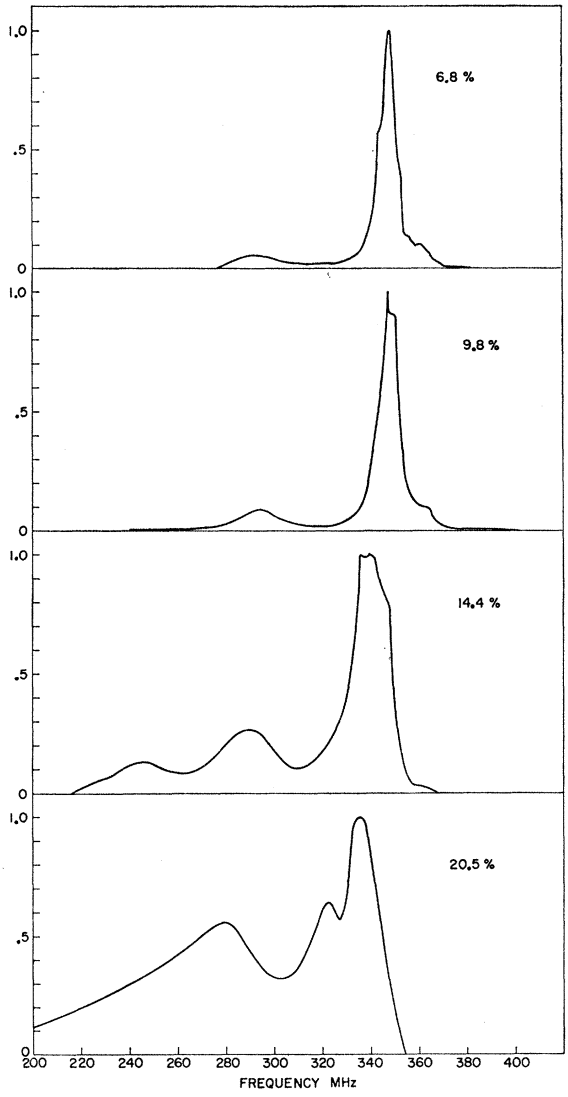

FIG. 2. Corrected Mn^{55} line shapes at 4.2°K in the higher concentration Ni-Mn alloys.

have been plotted versus concentration at the three temperatures.

D. Studies in Externally Applied dc Magnetic Fields

We have also studied the 0.8% alloy at room temperature in external dc magnetic fields of up to 10 kG, using higher rf power and longer pulse widths. The results are shown in Fig. 6. In fields above about 2.5

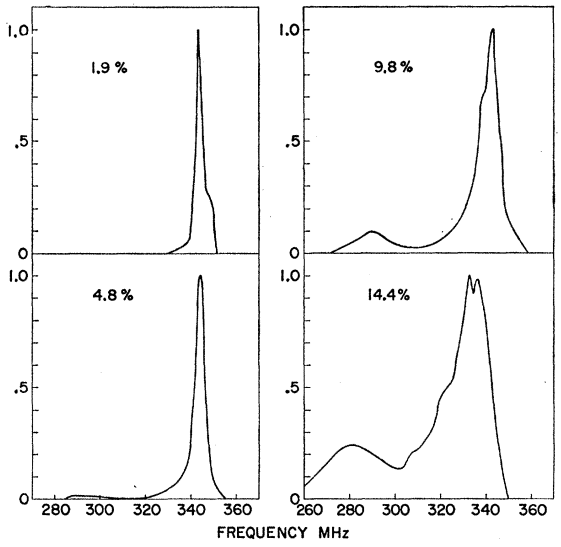

FIG. 3. Corrected Mn^{55} line shapes at 77°K in the Ni-Mn alloys.

kG, the frequency decreases with external field at the rate of 10.4±0.3 MHz per 10 kG, indicating a negative hyperfine field. The results are similar (if one takes into account the difference in nuclear moments of Mn^{55} and Ni^{61}) to those found in pure Ni metal.[17] The sign of the

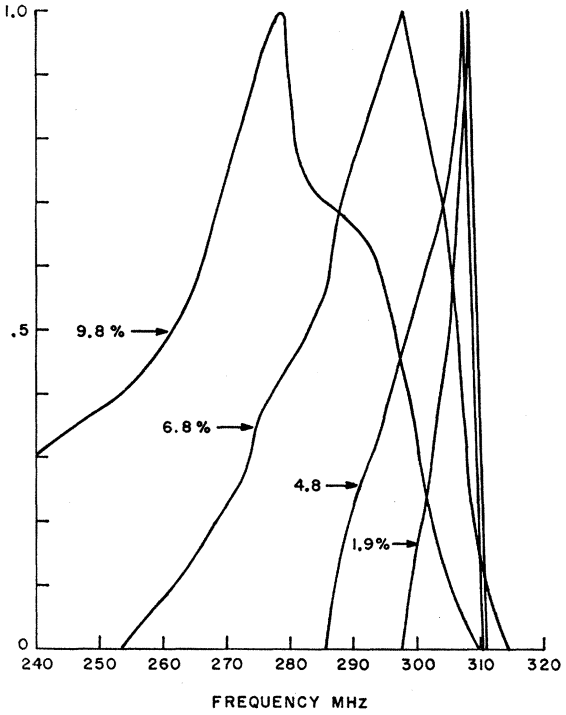

FIG. 4. Corrected Mn^{55} line shapes at room temperature in the Ni-Mn alloys.

[17] R. L. Streever, Phys. Rev. Letters **10**, 232 (1963).

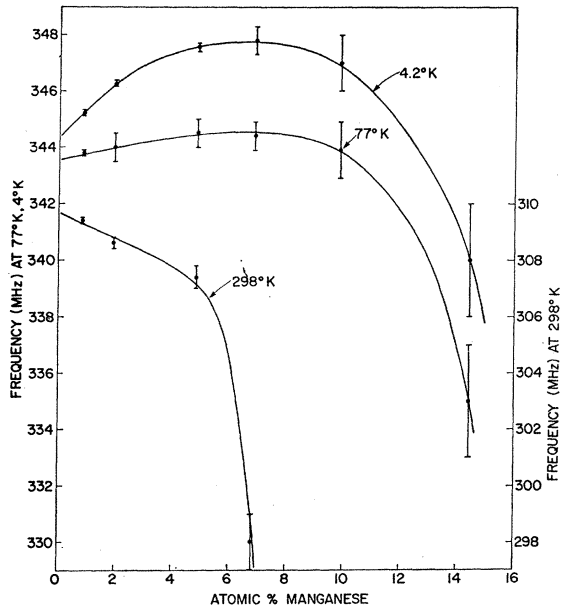

FIG. 5. Frequency of the peak of the main resonance line plotted against Mn concentration at various temperatures.

field is in agreement with the recent results of Cameron *et al.*[18] The value 10.4±0.3 for the frequency-field ratio of Mn^{55} is in good agreement with a recent ENDOR value of 10.500±0.007 MHz per 10 kG.[19]

E. Relaxation Times

For the zero-field studies, the relaxation times were from nuclei in domain walls and were nonexponential and dependent on the rf power level used. In the dilute alloy, the initial transverse relaxation time T_2 at low power levels was about 200 μsec at 4.2°K. T_2 decreased with increasing Mn concentration to a value of about 10 μsec in the 14.4% alloy. At the higher concentrations T_2 became nearly exponential and less dependent on rf power and was probably determined by Mn nuclear spin-spin interactions. To obtain the correct line shapes, it was necessary to take into account the variation of T_2 with frequency. In the dilute alloy, since the echo signal could be observed at a time which was short compared with T_2, the T_2 correction was small. It was found that in the higher-concentration alloys T_2 was nearly independent of frequency for any given sample.

III. DISCUSSION

A. Discussion of Magnetic Measurements

Before discussing the hyperfine fields, we will consider the magnetic properties of the Ni–Mn alloys. For Mn atoms surrounded only by Ni nearest neighbors the Mn atoms should be ferromagnetically aligned, as already discussed. As the Ni nearest neighbors become replaced by ferromagnetically aligned Mn neighbors, a point will be reached where the negative Mn–Mn interactions overpower the Ni–Mn interactions and the central Mn moment becomes antiferromagnetically aligned with respect to its neighbors. This model has been used by Marcinkowski and Poliak[7] to explain the change of magnetization with ordering in Ni_3Mn. Using reasonable values for the relative magnitudes of the various exchange interactions involved, Marcinkowski and Poliak conclude that a Mn moment will be antiferromagnetically aligned when it has three or more ferromagnetically aligned Mn nearest neighbors. In order to test this model, we will use it to calculate the magnetization of the alloy system as a function of Mn concentration.

The average magnetic moment of the alloy $\bar{\mu}$ can be written as

$$\bar{\mu}=\mu_{\mathrm{Mn}}(c_{\mathrm{Mn}\uparrow}-c_{\mathrm{Mn}\downarrow})c+\mu_{\mathrm{Ni}}(1-c). \qquad (1)$$

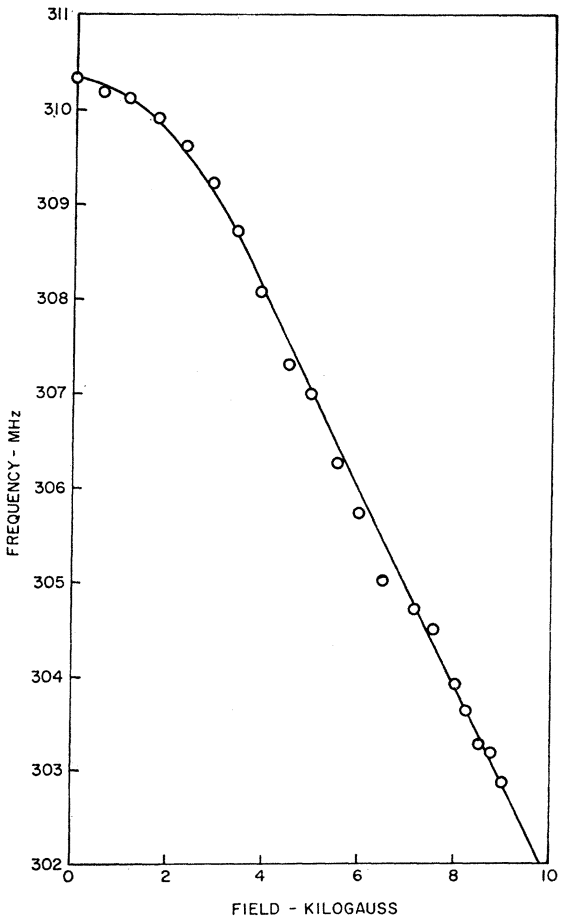

FIG. 6. External dc magnetic field dependence of resonance frequency at room temperature in an alloy of 0.8% Mn in Ni.

[18] J. A. Cameron *et al.*, Proc. Phys. Soc. (London) **90**, 1077 (1967).
[19] W. B. Mins *et al.*, Phys. Letters **24A**, 481 (1967).

Here $c_{Mn\uparrow}$ and $c_{Mn\downarrow}$ are the fractional number of Mn atoms at each concentration with magnetic moments along and against $\bar{\mu}$, respectively, c is the fractional Mn concentration, and μ_{Ni} and μ_{Mn} are the average Ni and Mn moments.

Let c_N be the fractional number of Mn atoms with N Mn nearest neighbors, where N varies from zero to 12. For various Mn concentrations we have calculated c_N statistically, using the binomial distribution. We have calculated $c_{Mn\uparrow}$ and $c_{Mn\downarrow}$ by assuming $c_{Mn\uparrow}=c_0+c_1+c_2$ and $c_{Mn\downarrow}=1-c_{Mn\uparrow}$. Then taking $\mu_{Mn}=3.0\ \mu_B$ and $\mu_{Ni}=0.6\ \mu_B$ (independent of concentration), we have calculated $\bar{\mu}$ from Eq. (1). Values of $c_{Mn\uparrow}$, $c_{Mn\downarrow}$, and $\bar{\mu}$ calculated in this manner are given in Table I for various fractional Mn concentrations c.

In Fig. 7 we have compared the calculated magnetic moments per atom with experimental data from the literature. The experimental data we have used are mainly those of Sadron.[1] In this concentration range, measurements are reported in the literature on both ordered and disordered alloys.[2–4] Sadron's data up to about 20% Mn are in general agreement with the disordered-alloy data of Refs. 2–4. In the concentration range around the Ni_3Mn concentration, a great amount of recent magnetization data exist (see Refs. 5–7 and the references contained therein). We have plotted on Fig. 7 a point from Ref. 6 where the measurements were made on an almost completely disordered alloy at 4.2°K. This point is in approximate agreement with an extrapolation of Sadron's lower-concentration data. From Fig. 7 the magnetization should go to near zero at about 30% Mn, in agreement with Ref. 5. The experimental curve of Fig. 7 should then be a reasonably good representation of the magnetization in the disordered alloys. The agreement between the calculated and experimental magnetization curves is quite good, considering the assumptions made and the crudeness of the model. The success of the model probably lies in the fact that it predicts the Mn moments to be paired off near the Ni_3Mn concentration. This would be required for the energy to be a minimum if the Mn–Mn

TABLE I. Tabulation of $c_{Mn\uparrow}$ and $c_{Mn\downarrow}$, the fractional number of Mn atoms with moments parallel and antiparallel to the net magnetization, respectively, for various fractional Mn concentrations c (see text). The last column shows values of $\bar{\mu}$ calculated by Eq. (1) assuming 3 μ_B for μ_{Mn} and 0.6 μ_B for μ_{Ni}.

c	$c_{Mn\uparrow}$	$c_{Mn\downarrow}$	$\bar{\mu}$ (μ_B)
0.00	1.000	0.000	0.600
0.02	0.999	0.001	0.648
0.05	0.980	0.020	0.714
0.07	0.953	0.047	0.748
0.10	0.889	0.111	0.773
0.15	0.735	0.265	0.722
0.20	0.557	0.443	0.548
0.25	0.391	0.609	0.287

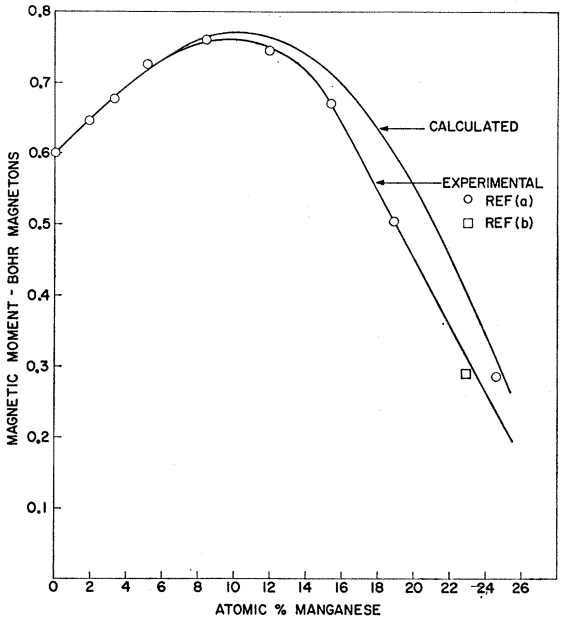

FIG. 7. A comparison of the magnetization of the Ni–Mn alloy system as calculated by Eq. (1), with experimental data of Refs. 1(a) and 6(b).

interaction is dominant.[9] In the following discussion of hyperfine fields we will assume the preceding model to apply. The assumption of concentration-independent moments is only approximate (neutron-diffraction data[20] in ordered Ni_3Mn give $\mu_{Mn}=3.2\ \mu_B$ and $\mu_{Ni}=0.3\ \mu_B$). If, however, we were to assume the Mn moments to be exactly paired off at 25% Mn and took $\mu_{Ni}=0.3\ \mu_B$, then from Eq. (1) we would obtain a $\bar{\mu}$ of 0.22 μ_B close to the experimental value. In the ordered Ni_3Mn alloy, however, we would have (since all moments are ferromagnetically aligned), with $\mu_{Mn}=3.2\ \mu_B$ and $\mu_{Ni}=0.3\ \mu_B$, a $\bar{\mu}$ of 1.0 μ_B, also in agreement with experiment.

B. Discussion of Nuclear-Resonance Results

If we consider the experimental results at 4.2°K, we see that at low concentrations of Mn, in addition to the main line at 347 MHz, a high-frequency satellite line appears at about 360 MHz and a broad low-frequency line at about 290 MHz. At higher Mn concentrations a broad line develops at around 250 MHz. The line at 290 MHz has the intensity at each concentration that one would expect statistically if all the Mn atoms with 3-Mn nearest neighbors and about $\frac{1}{3}$ of the Mn atoms with 2-Mn nearest neighbors were assumed to contribute to it. The line at 250 MHz has a somewhat greater intensity than one would expect from Mn atoms with 4-Mn nearest neighbors. We assume then that most Mn atoms with less than 3-Mn nearest

[20] C. G. Shull and M. K. Wilkinson, Phys. Rev. 97, 304 (1955).

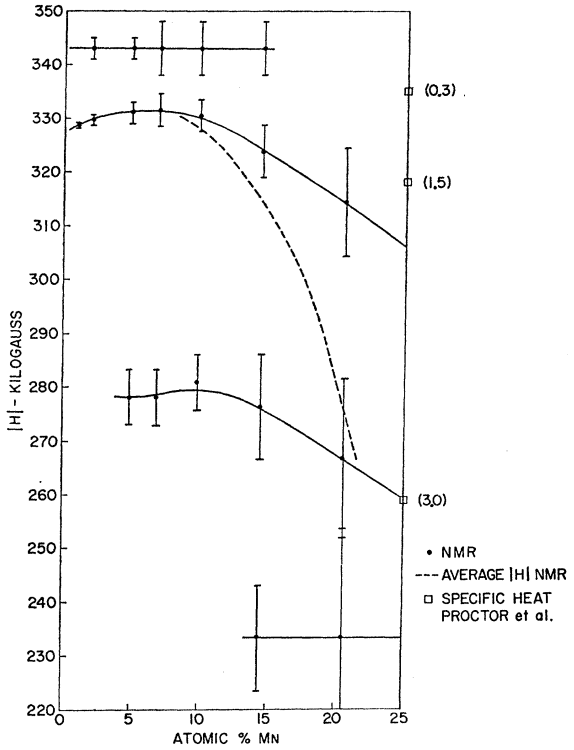

FIG. 8. A plot of the absolute magnitude of the Mn hyperfine fields associated with the principal lines. Also plotted is the average magnitude of the hyperfine field determined from the center of gravity of the frequency distributions. Hyperfine fields in Ni_3Mn (from Ref. 13) corresponding to various average numbers of Mn nearest neighbors are also indicated.

neighbors are contributing to the main line and the satellite at 360 MHz, while the lines at 290 and 250 MHz arise mainly from Mn atoms with 3 or more Mn nearest neighbors. In Fig. 8 we have plotted the absolute magnitude of the hyperfine fields at 4.2°K associated with the principal lines assuming a frequency-field relationship of 10.5 MHz/(10 kG). Also plotted is the average magnitude of the hyperfine field determined from the center of gravity of the frequency distributions.

From low-temperature specific-heat measurements Proctor *et al.*[13] have obtained hyperfine-field values at Mn^{55} in Ni_3Mn for various degrees of order. Since varying the degree of short-range order changes the average number of Mn nearest neighbors, their results can be compared with ours. In Fig. 8 we have plotted the hyperfine fields obtained from the specific-heat results in Ni_3Mn corresponding to 0.3-, 1.5-, and 3.0-Mn nearest neighbors (on the average). Only the point for the completely disordered alloy (corresponding to 3.0-Mn nearest neighbors) can be compared with our results. We see, however, that our interpretation of the nuclear resonance is in generally good agreement with the specific-heat results and that the average hyperfine field extrapolated to 25% Mn is in approximate agreement with the specific-heat value for disordered Ni_3Mn.

Specific-heat measurements have also been made in Ni_3Mn by Stetsenko and Avksentev.[14] Their measurements indicate a hyperfine field in the disordered Ni_3Mn alloy of 340 kG, considerably higher than the value of 259 kG found by Proctor *et al.* and higher than the one which we find in the 20% alloy. The discrepancy in the specific-heat data appears, however, to be due to the method of fitting the heat-capacity–versus–temperature curves rather than in the experimental data themselves and our results would appear to show the fit of Proctor *et al.* to be the correct one.

C. Discussion of Hyperfine Fields in Alloys

As in previous discussions of hyperfine fields in Ni alloys,[15,16] we will use a phenomenological approach and try to fit the hyperfine fields to an expression of the following form:

$$H_A = a\mu_A + b\bar{\mu}. \tag{2}$$

Here the first term in (2) represents the contribution to the hyperfine field at the nucleus of atom A from the magnetic moment μ_A of the parent atom, and $\bar{\mu}$ can be taken to be the average magnetic moment of the alloy or in some cases, in a more detailed treatment, the average moment of neighboring atoms. Previous studies of Ni alloys indicate that a and b are both negative and of comparable magnitude.

We will now discuss Eq. (2) qualitatively. Consider first the dilute alloy. For Mn atoms with only Ni nearest neighbors, since μ_A is positive with respect to $\bar{\mu}$ and a and b are both negative, the hyperfine field should be negative, in agreement with the external-field studies. For clusters of ferromagnetically coupled Mn atoms such as Mn pairs, $\bar{\mu}$ should increase and H_A should increase in absolute magnitude, resulting in satellite lines on the high-frequency side of the main line. The satellite line at 360 MHz is probably due to pairs of nearest- or next-nearest-neighbor Mn atoms which are ferromagnetically coupled to $\bar{\mu}$. Mn atoms with 3 or more Mn nearest neighbors, however, should be antiferromagnetically aligned with respect to the neighbors and with respect to $\bar{\mu}$ of the alloy and in this case, since μ_A and $\bar{\mu}$ are of opposite sign, the absolute magnitude of H_A should be reduced as is observed.

If we interpret $\bar{\mu}$ in Eq. (2) as being that of the alloy, then in the dilute alloy the difference in hyperfine fields for Mn atoms with moments parallel and antiparallel to $\bar{\mu}$ should be just $2b\bar{\mu}$. Equating this to the hyperfine-field difference between the main line and the line at 290 MHz gives a value for $2b\bar{\mu}$ of about -50 kG. Taking $\bar{\mu}=0.6\ \mu_B$, we obtain for b a value of -42 kG/μ_B. Then with $\mu_A=3.0\ \mu_B$ and $H_A=-330$ kG, we obtain from Eq. (2) $a=-102$ kG/μ_B. These values of a and b are close to those obtained previously in studies of Ni-rich

TABLE II. Spin configurations associated with various numbers N of Mn nearest neighbors surrounding a central Mn atom. Values of μ_A, the moment of the central Mn atom, and $\bar{\mu}$ (nn), the average moment of nearest-neighbor shell, are given (see text). Values of H_A calculated from Eq. (4) and the corresponding frequencies are given.

N	Configuration	$\mu_A(\mu_B)$	$\bar{\mu}$(nn) (μ_B) [Eq. (3)]	H_A[Eq. (4)] (kG)	ν(MHz) $=1.05\mid H_A\mid$
2	↑-↑ ↑	3.0	1.0	−350	368
1	↑-↑	3.0	0.8	−340	357
0	↑	3.0	0.6	−330	347
2	↑-↑ ↓	3.0	0.5	−325	341
1	↑-↓	3.0	0.3	−315	331
2	↑-↓ ↓	3.0	0.0	−300	315
3	↑-↓ ↓ ↓	3.0	−0.3	−285	299
3	↓-↑ ↑ ↑	−3.0	1.2	240	252
4	↓-↑ ↑ ↑ ↑	−3.0	1.4	230	242

alloys.[16] As discussed in Ref. 16, Eq. (2) with approximately the above values of a and b predicts approximately the values of hyperfine fields for various transition elements in Ni. The value of a is also close to the value Watson and Freeman[21] suggest in estimating the core-polarization contribution to H_A.

Alternatively, if we consider the effects on H_A from atoms in the nearest-neighbor shell to atom A to be the most important, we can interpret $\bar{\mu}$ in Eq. (2) as being the average moment of the nearest-neighbor shell. We will now calculate H_A using this approach, which is similar to that used in Ref. 13. The average moment $\bar{\mu}$ (nn) of the nearest-neighbor shell can be written as

$$\bar{\mu}\,(\mathrm{nn})=\tfrac{1}{12}[(12-N)\mu_{\mathrm{Ni}}+N\mu_{\mathrm{Mn}}], \qquad (3)$$

where N is the number of Mn nearest neighbors. We have taken μ_{Ni} to be 0.6 μ_B and μ_{Mn} to be ± 3.0 μ_B, according to whether the Mn moment is aligned with or against the net magnetization $\bar{\mu}$. Values of $\bar{\mu}$ (nn) calculated by use of Eq. (3) for various configurations of Mn nearest neighbors surrounding a central Mn atom are shown in Table II. The symbol ↑-↓ ↓ refers to the case of the moment of the central Mn atom being along $\bar{\mu}$, with the moments of the two nearest-neighboring Mn atoms being coupled antiferromagnetically to it. We have then calculated H_A, the hyperfine field at the central Mn atom, by taking

$$H_A=-100\,\mu_A-50\bar{\mu}\,(\mathrm{nn}). \qquad (4)$$

Here H_A is in kG and μ is in Bohr magnetons.

The constants in Eq. (4), which are approximately the same as those obtained in the preceding discussion, have been chosen to give approximate agreement between the experimental and calculated hyperfine fields. Since we are following the usual convention of taking H_A to be positive when it lies along the direction of $\bar{\mu}$ (or the direction of an externally applied magnetic field), we must take μ_A in Eq. (4) to be positive when it lies along $\bar{\mu}$ and negative otherwise. Values of H_A calculated by use of Eq. (4) are given in Table II together with the corresponding resonance frequencies.

The hyperfine-field values expected for the various configurations agree approximately with those observed experimentally. From Table II we see that the line associated with the configuration ↑-↑ should occur at about 357 MHz, suggesting that the line at 360 MHz may be from this configuration. The configuration ↑-↑ ↑ may be contributing to the high-frequency tail which extends up to about 400 MHz. At higher Mn concentrations, however, the Mn atoms should be roughly paired off so that Mn atoms should see predominantly antiferromagnetically coupled Mn nearest neighbors. Consequently, at the higher concentrations lines associated with the configurations ↑-↑ and ↑-↑ ↑ would be expected to decrease in intensity, while intensity would be expected to build up on the low-frequency side of the main line due to the configurations ↑-↓ and ↑-↓ ↓. This is observed experimentally.

The lines at 290 and 250 MHz which we previously associated with Mn atoms with 3- and 4-Mn nearest neighbors probably arise from the configurations ↓-↑ ↑ ↑ and ↓-↑ ↑ ↑ ↑, although configurations such as ↑-↓ ↓ ↓ would also be expected to occur at the higher concentrations. In the 20.5% alloy the low-frequency peak should be mainly from Mn atoms with moments pointing against $\bar{\mu}$, while the high-frequency peak should be mainly from moments pointing along $\bar{\mu}$. The fact that the integrated intensities of these two peaks are of comparable magnitude is in agreement with our previous considerations that the Mn moments should be about equally paired off at this concentration.

D. Long-Range Effects

Although a Mn moment of 3.0 μ_B is needed to explain the magnetic measurements in the dilute alloy (assum-

[21] R. E. Watson and A. J. Freeman, Phys. Rev. **123**, 2027 (1961).

ing a Ni moment of 0.6 μ_B) and this value was used in the preceeding calculation, there is some evidence from recent neutron-diffraction studies in the dilute alloy that the Mn moment has a value somewhat less than this. Collins and Low[22] have recently used neutron scattering techniques to study dilute alloys of Mn in Ni. They find the Mn moments to be well localized, with moments 1.8 μ_B greater than those of the host corresponding to $\mu_{Mn}=2.4\ \mu_B$, $\mu_{Ni}=0.6\ \mu_B$. This result is in disagreement with the magnetic measurements where an effective manganese moment of 3.0 μ_B is needed to explain the results at low Mn concentrations. One explanation for the disagreement suggested by Collins and Low is that at low temperatures there is a long-range increase in moments on all lattice sites due to the addition of Mn. If we examine Fig. 5, we see that in addition to the localized effects we have discussed there is a shift of the peak of the Mn resonance line at low concentrations. At 4.2°K the shift is to higher frequency, with increasing Mn concentration, corresponding to an increase in moments. This is a long-range effect [even the 0.8% Mn alloy (not shown in Fig. 1) showed an asymmetry to higher frequencies, indicating the range of the effect to be several neighbor shells]. By use of Eq. (4), assuming an increase in moments at *all* lattice sites, we can relate the frequency shift to the long-range moment change.

If we let $(d\mu/dc)'$ be the change of magnetic moments with fractional Mn concentration c, we have from Eq. (4)

$$dv/dc=1.05d\,|\,H_A\,|/dc$$
$$=(1.05)\,(150)\,(d\mu/dc)'. \qquad (5)$$

In Eq. (5) dv/dc is in MHz and $(d\mu/dc)'$ is in Bohr magnetons. From Fig. (5) we obtain at 4.2°K at low concentrations a value for dv/dc of 97±25 MHz. Using this value in Eq. (5) gives a $(d\mu/dc)'$ of 0.6±0.1 μ_B.

The total $d\bar{\mu}/dc$ will be given by

$$d\bar{\mu}/dc=\mu_{Mn}-\mu_{Ni}+(d\mu/dc)'. \qquad (6)$$

Using in Eq. (6) a $d\bar{\mu}/dc$ of 2.4 μ_B (from the magnetic measurements at low temperatures), a μ_{Ni} of 0.6 μ_B, and a $(d\mu/dc)'$ of 0.6 μ_B gives for μ_{Mn} a value of 2.4 μ_B, in agreement with the results of Collins and Low.

A similar calculation at room temperature, using the room-temperature curve of Fig. 5, gives a $(d\mu/dc)'$ of about $-0.3\ \mu_B$. Using this value in Eq. (6) gives a $d\bar{\mu}/dc$ of about 1.5 μ_B, which is in approximate agreement with the magnetic measurements at room temperature.

[22] M. F. Collins and G. G. Low, Proc. Phys. Soc. (London) 86, 535 (1965).

E. Temperature Effects

Using the model discussed previously in Sec. III A, it is clear that Mn atoms with only Ni nearest neighbors will be strongly coupled to the lattice. The coupling will be weaker for Mn atoms with one ferromagnetically coupled Mn nearest neighbor and weaker still for atoms with two ferromagnetically coupled Mn neighbors. Consequently, we expect the high-frequency lines to shift to lower frequency with increasing temperature more rapidly than the main line. The satellite which appears at 360 MHz at 4.2°K may have actually shifted into the main line at 77°K. The strong asymmetry to lower frequencies which occurs at room temperature is probably also a consequence of the above effects. In the 14.4% alloy, the frequency of the peaks which occur at 340 and 290 MHz at 4.2°K both decrease by about 1.5% in going to 77°K. Since the Curie temperature of this sample is about 420°K, a shift of this magnitude seems quite reasonable.

IV. CONCLUSIONS

The magnetic moments and the hyperfine fields in the Ni–Mn alloy system can be consistently explained by taking into account the antiferromagnetic interactions in these alloys and by assuming the hyperfine fields to be composed of two contributions, one contribution from the moment of the parent atom and one from neighboring atoms. The sign and approximate magnitudes of the two contributions are in approximate agreement with those found for Ni-rich alloys previously.

Although the Mn moment appears for the most part to be quite well localized, we have found in addition to the localized effects a shift in the Mn hyperfine field resulting from distant Mn atoms. By assuming a long-range increase in magnetic moments due to the addition of Mn, one can consistently explain both the NMR shift and the discrepancy of recent neutron scattering experiments with the magnetic measurements.

It would be interesting in further studies of the Ni–Mn alloys to examine the Ni^{61} resonance, particularly at low Mn concentrations. Also, a study of the Mn^{55} resonance in concentrations around Ni_3Mn in both atomically ordered and atomically disordered alloys would be interesting.

Finally, studies of the Mn^{55} resonance in the higher-concentration alloys with an externally applied dc field would be useful in order to verify that the signs of the hyperfine fields of the lower-frequency satellites are indeed positive. Studies in these areas are presently in progress.

ACKNOWLEDGMENT

The author wishes to thank A. J. Montedoro for his technical assistance.